

# **LSD1 controls a nuclear checkpoint in Wnt/ $\beta$ -Catenin signaling to regulate muscle stem cell self renewal**

Sandrine Mouradian,<sup>1,4</sup> Delia Ciccirello,<sup>1,4</sup> Nicolas Lacoste,<sup>1</sup> Francesca Berretta,<sup>1</sup> Fabien Le Grand,<sup>2</sup> Nicolas Rose,<sup>2</sup> Laurent Schaeffer,<sup>1,3\*</sup> Isabella Scionti<sup>1,\*</sup>

<sup>1</sup> Pathophysiology and Genetics of Neuron and Muscle (PGNM), Institut NeuroMyoGène, Université Claude Bernard Lyon 1, CNRS UMR5261, INSERM U1315, Faculté de Médecine Rockefeller, France

<sup>2</sup> Sorbonne Université, UPMC Université Paris 06, INSERM UMRS974, CNRS FRE3617, Center for Research in Myology, 75013 Paris, France

<sup>3</sup> Centre de Biotechnologie Cellulaire, Hospices Civils de Lyon, groupement Est, Bron, France

<sup>4</sup> These authors contributed equally.

\* Correspondence: [isabella.scionti@inserm.fr](mailto:isabella.scionti@inserm.fr), [laurent.schaeffer@univ-lyon1.fr](mailto:laurent.schaeffer@univ-lyon1.fr)

## **Abstract**

The Wnt/ $\beta$ -Catenin pathway plays a key role in cell fate determination during development and in adult tissue regeneration by stem cells. These processes involve profound gene expression and epigenome remodeling and linking Wnt/ $\beta$ -Catenin signaling to chromatin modifications has been a challenge over the past decades. Functional studies of the histone demethylase KDM1a/LSD1 converge to indicate that this epigenetic regulator is a key regulator of cell fate <sup>1</sup>, although the extracellular cues controlling LSD1 action remain largely unknown. Here we show that  $\beta$ -Catenin is a substrate of LSD1. Demethylation by LSD1 prevents  $\beta$ -Catenin degradation thereby increasing its nuclear levels. In muscle stem cells,  $\beta$ -Catenin and LSD1 are both recruited on the *MyoD* Core Enhancer to control *MyoD* expression and promote muscle stem cell commitment <sup>2,3</sup>. Moreover, a  $\beta$ -Catenin reporter construct shows that the involvement of LSD1 in  $\beta$ -Catenin regulation is not restricted to *MyoD* activation. Altogether, by inscribing them in the same molecular cascade linking extracellular factors to epigenetic modifications and gene expression, our results provide a rational explanation to the similarity of action of canonical Wnt signaling and LSD1 on cell fate.

## **Introduction**

Resident quiescent muscle stem cells (MuSCs) confer skeletal muscle unique regenerative capacities and play a central role in skeletal muscle plasticity. While quiescent under resting conditions, upon muscle injury MuSCs activate a specific cascade of transcription factors, leave the quiescent state, expand and further differentiate into myocytes, before maturing into myofibers. Notably, a subset of activated MuSCs resists the differentiation process, thereby returning in quiescence to replenish the pool of MuSCs <sup>4-7</sup> sufficient to support future rounds of muscle growth/regeneration. The control of the balance between MuSC commitment and self-

renewal is crucial for muscle homeostasis and the fine tuning of *MyoD* expression plays a key role to set this balance<sup>8</sup>.

We have previously shown that LSD1 is crucial for the timely activation of *MyoD* expression during the commitment of muscle progenitors, via the activation of the Core Enhancer region (CER) of the *MyoD* gene<sup>3</sup>. Consistently, LSD1 ablation delays *MyoD* expression during embryonic myogenesis. However, none of the histone modifications occurring on the CER upon activation can be directly attributed to LSD1 enzymatic activity<sup>3</sup>, thus raising the question of its actual role in CER activation.

The function of canonical Wnt/ $\beta$ -catenin signaling in regulating MuSCs homeostasis has been extensively studied over the past decade. In the absence of Wnt ligands,  $\beta$ -catenin is phosphorylated in the cytosol by the destruction complex (mainly composed by Axin, Adenomatous Polyposis Coli and the Glycogen Synthase Kinase 3  $\beta$ ), which triggers its ubiquitination and rapid degradation by the proteasome. Activation of Wnt/ $\beta$ -catenin signaling is required for myogenesis since disruption of Wnt/ $\beta$ -catenin signaling or  $\beta$ -catenin mutations cause muscle developmental and regenerative defects<sup>9</sup>. In MuSCs, upon binding of Wnt ligands to their receptor, the destruction complex is inhibited, thus preventing  $\beta$ -catenin phosphorylation and degradation.  $\beta$ -catenin is then methylated by the methyltransferase SETD7<sup>10</sup> to allow its translocation into the nucleus to participate to the engagement of MuSCs into differentiation.

## Results

### LSD1 inactivation increases MuSC self-renewal potential.

To investigate the role of LSD1 in adult MuSCs, LSD1 was specifically inactivated in MuSCs using LSD1 conditional Knock-Out mice expressing a tamoxifen-inducible CRE-recombinase under the control of the *Pax7* promoter (*Pax7-CreERT2:Lsd1<sup>tm1Schüle</sup>*, hereafter named LSD1 SCiKO mice). 10 weeks old mice were treated with tamoxifen (TAM), and MuSCs were FACS-isolated 1 week later. MuSCs isolated from *Pax7-CreERT2* mice treated with TAM (hereafter named CTRL SC) were used as a control (Supplementary Fig. 1a). A high degree of recombination was evident in FACS-purified MuSCs from LSD1 SCiKO mice based on the amount of LSD1 protein level (Supplementary Fig. 1b). As previously reported the ablation of LSD1 did not impact the proliferation rate of MuSCs *in vitro* (Supplementary Fig. 1c). After 2 days in myogenic differentiation medium (MDM) LSD1 SCiKO MuSCs displayed impaired myogenesis as evidenced by a strong reduction in the proportion of Myogenin positive (+) cells compared to CTRL SC MuSCs (Supplementary Fig. 1d). Conversely, the proportion of PAX7+ cells was significantly increased in LSD1 SCiKO MuSCs compared to CTRL SC MuSCs (Fig. 1a). This increase was caused by the loss of LSD1 enzymatic activity since the LSD1

pharmacological inhibitors Pargyline and OG-L002 produced the same effect on control MuSCs (Fig. 1b). Altogether, these results suggested that the loss of LSD1 delayed MuSC commitment as we previously showed for myogenic progenitors during development<sup>3</sup>. Reduced myogenesis could not be attributed to activation of the adipogenic program, since LSD1 SCiKO MuSCs did not produce lipid-containing mononucleated cells in MDM (Fig. 1c). We next examined the effect of LSD1 inactivation on MuSCs *in vivo*. *Lsd1* gene inactivation did not affect the number of quiescent MuSC in healthy muscles, as shown by PAX7 immunofluorescence on *Tibialis Anterior* (TA) muscle cryosections (Supplementary Fig. 2 a-b). Of note, 7 and 56 days after the last TAM injection, the number of fibers per mm<sup>2</sup> and the histological features (Supplementary Fig. 2 c-d) were also similar in LSD1 SCiKO and CTRL SC uninjured TA muscles. To investigate LSD1 role during muscle regeneration, TA muscles of LSD1 SCiKO and CTRL SC were injured by cardiotoxin (CTX) injection. Seven days after CTX injury (Supplementary Fig. 2e), LSD1 SCiKO TA muscles displayed smaller regenerating fibers than CTRL SC TA muscles (Supplementary Fig. 2 f-g). Consistently with the *in vitro* results, we did not observe an increase in adipocyte-like cells (Supplementary Fig. 2h). Surprisingly, 28 days post injection (dpi) (Fig. 1d), when muscles were completely regenerated and MuSCs had returned into quiescence, the number of PAX7+ cells per mm<sup>2</sup> was increased by 50% in LSD1 SCiKO muscles compared to CTRL SC (Fig. 1e). Staining for PAX7 and the proliferation marker Ki67 showed that in both conditions more than 95% of the PAX7+ cells were negative for Ki67, indicating that they were not proliferating (Supplementary Fig. 2i). Evaluation of regeneration 28 dpi showed that the number of fibers per mm<sup>2</sup> and the distribution of myofiber cross sectional area (CSA) were similar in CTRL SC and LSD1 SCiKO TA muscles (Fig. 1 f-g). Altogether, these results indicated that in the absence of LSD1, MuSC self-renewal is increased but the regenerative potential of muscle is preserved *in vivo*.

To investigate whether pharmacological inhibition of LSD1 produced similar effects, *wild-type* (WT) mice were treated with the pharmacological inhibitor of LSD1 (OG-L002<sup>11</sup>) and TA muscles were injured by CTX injection (Fig. 1h). Twenty-one dpi, the number of quiescent MuSCs (PAX7+/Ki67-) in TA muscles was significantly higher in mice treated with OG-L002, compared to vehicle (Fig. 1i). The histological analysis and the number of fibers per mm<sup>2</sup> showed no significant differences between treated and untreated mice (Fig. 1 j-k). These results support the conclusion that the effect of LSD1 inactivation on MuSC self-renewal is due to the loss of LSD1 enzymatic activity.

## **LSD1 inactivation enhances MuSC regenerative potential after repeated injury**

Since LSD1 ablation or inhibition increased the pool of MuSCs, we hypothesized that it could either be beneficial or detrimental for further regeneration events. Three consecutive muscle regenerations were therefore performed by three successive CTX injections 28 days apart from each other in LSD1 SCiKO and CTRL SC TA muscles. Injured muscles were analyzed 7 and 28 days after the third CTX injection (dpIII, Fig. 2a). Surprisingly, fiber number per mm<sup>2</sup> were not reduced anymore at 7 dpIII in LSD1 SCiKO conversely to what was observed after a single round of regeneration (Fig. 2b and Supplementary Fig. 2f). In addition, regeneration efficiency at 28 dpIII was similar to what was observed after a single CTX injection in CTRL SC: the distribution of regenerated fibers CSA, the number of fibers for mm<sup>2</sup> as well as the histological analysis was similar between CTRL SC and LSD1 SCiKO mice (Fig. 2 b-d) but a 40% increase in the number of MuSCs/mm<sup>2</sup> in LSD1 SCiKO mice compared to CTRL SC was still present (Fig. 2e). These results indicated that the loss of LSD1 in MuSCs both increased the pool of PAX7+ while preserving the regenerative potential of muscles even after repeated injuries.

## **LSD1 inactivation stimulates symmetric division.**

To better understand the mechanism underlying this phenotype, we investigated at which specific stage LSD1 inactivation affected MuSC division *in vivo*. After muscle injury, MuSCs undergo a first round of division between 28 and 40 hours (h) <sup>12,13</sup>. A pulse labeling of mitosis was performed by injecting the deoxynucleotide analog EdU 28 h post injury (hpi). MuSCs were isolated 12 h later (40 hpi) (Fig. 3a). In absence of LSD1, MuSCs activated as well as the control ones (Fig. 3b). After completing the first round of division MuSCs rapidly proliferate to expand their number to allow the repair of the muscle. To measure the rate of MuSC expansion, muscles were analyzed by immunostaining PAX7, Ki67 and EdU incorporation at 96 h post injury (Fig. 3 a-c). No difference was observed between the proliferation rate of CTRL SC and LSD1 SCiKO MuSCs (Fig. 3c). As expected, the absolute number of PAX7+ cells was already significantly increased in absence of LSD1 (Fig. 3d). MuSCs can undergo either planar symmetric division to give rise to two MuSCs (to increase the pool) or alternatively undergo an asymmetric division to give rise to a stem cell and a committed one. Altogether, our data suggested that LSD1 might be involved in the regulation of the balance between symmetric and asymmetric MuSC first division. To test whether LSD1 regulated such Symmetric/Asymmetric division balance, myofibers were placed in culture for 42 h before immunostaining PAX7 and MYF5, as previously described <sup>14</sup>. In the absence of LSD1, the percentage of asymmetric divisions yielding one Pax7+/MYF5+ cell was drastically reduced to 2% compared to CTRL SC MuSCs that underwent 15% of

asymmetric division (Fig. 3e). These data indicated that LSD1 has a pro-differentiation action by favoring asymmetry during the first division of MuSCs.

### **LSD1 is required for transcriptional activation by $\beta$ -catenin.**

During development and to preserve tissue homeostasis, many types of stem cells rely on Wnt/ $\beta$ -catenin signaling to set the balance between self-renewal and differentiation by promoting asymmetric cell division<sup>15-19</sup>. In embryonic stem cells, Wnt-coreceptors and  $\beta$ -catenin control the orientation of the mitotic spindle to favor asymmetric division<sup>18</sup>. Since both LSD1 and  $\beta$ -catenin promote asymmetric division and since both were shown to activate the *MyoD* CER<sup>2,3</sup>, we investigated whether LSD1 function could be linked to Wnt/ $\beta$ -catenin signaling. Chromatin immunoprecipitation (ChIP) was performed to evaluate the potential role of LSD1 in  $\beta$ -catenin recruitment on the *MyoD* CER during myoblast commitment. As expected, in myoblast expressing control shRNA (shSCRA cells<sup>3</sup>),  $\beta$ -catenin was strongly enriched on the CER after 72 hours in myogenic differentiation medium. Conversely myoblasts expressing a LSD1 shRNA (shLSD1 cells<sup>3</sup>) failed to recruit  $\beta$ -catenin on the CER (Fig. 4a). This indicated that LSD1 is required for the recruitment of  $\beta$ -catenin on the *MyoD* CER.

To determine if LSD1 was globally required for  $\beta$ -catenin transcriptional activity in myoblasts, shLSD1 and shSCRA myoblasts as well as CTRL SC and LSD1 SCiKO primary MuSCs were transfected with a  $\beta$ -catenin reporter luciferase construct and treated with Wnt3A or LiCl<sup>20</sup> to activate Wnt/ $\beta$ -catenin signaling. In absence of LSD1 myoblasts displayed very low luciferase expression compared to control cells (Supplementary Fig. 3a). Next, we evaluated the effect of LiCl on the activation of  $\beta$ -catenin target genes and as expected, LiCl increased the expression of *Fst*, *Porcn* and *Axin2* in shSCRA cells whereas their expression was hardly increased in shLSD1 cells (Supplementary Fig. 3b).

To promote myogenic cells differentiation, the Wnt/ $\beta$ -catenin signaling required the formation of a complex between  $\beta$ -catenin and BCL9<sup>21</sup>. Proximity ligation assay (PLA) was used to evaluate the interaction between  $\beta$ -catenin and BCL9 in CTRL SC and LSD1 SCiKO MuSC treated with Wnt3A. The results indicated that significantly less  $\beta$ -catenin/BCL9 complexes were formed in LSD1 SCiKO than in CTRL SC MuSCs (Fig. 4b). Altogether, these results showed that LSD1 is required for the activation of gene expression by  $\beta$ -catenin in myogenic cells.

### **Demethylation by LSD1 is required for $\beta$ -catenin stabilization in the nucleus**

We next investigated the mechanism through which LSD1 promoted  $\beta$ -catenin activity. Analysis of shLSD1 and shSCRA nuclear extracts by western blot showed that  $\beta$ -catenin levels were significantly lower in shLSD1

than in shSCRA nuclei, whereas the levels of  $\beta$ -catenin transcript were similar in both cell lines (Supplementary Fig. 3c-d). A time-course experiment with cycloheximide (CHX) to evaluate the stability of  $\beta$ -catenin protein showed that  $\beta$ -catenin half-life was strongly reduced in shLSD1 cells compared to shSCRA cells (Fig. 4c). It was recently shown that the lysine 180 of  $\beta$ -catenin must be mono-methylated by SETD7 to shuttle into the nucleus<sup>10</sup>. In addition,  $\beta$ -catenin lysine 180 methylation was shown to destabilize the protein<sup>22</sup>. Consistently, the proteasome inhibitor MG132 was more efficient to accumulate a non-methylable SETD7  $\beta$ -catenin mutant ( $\beta$ -CAT K180R) than WT  $\beta$ -catenin (Supplementary Fig. 3e). Co-immunoprecipitation experiments indicated that either over-expressed  $\beta$ -catenin and LSD1 or endogenous  $\beta$ -catenin and LSD1 co-immunoprecipitated (Supplementary Fig. 3f-g). We thus speculated that LSD1 directly demethylates  $\beta$ -catenin to stabilize it in the nucleus.  $\beta$ -catenin methylation was thus evaluated by western blot with an anti-pan methyl lysine (KpanMe) antibody on  $\beta$ -catenin immunoprecipitated from shSCRA or shLSD1 nuclear extracts. After 72h in myogenic differentiation medium, nuclear  $\beta$ -catenin methylation was very low in shSCRA nuclei whereas nuclear  $\beta$ -catenin remained strongly methylated in shLSD1 nuclei, suggesting that in the absence of LSD1 nuclear  $\beta$ -catenin was not demethylated during myoblast commitment (Fig. 4d). Finally, an *in vitro* de-methylation assay was performed with recombinant LSD1 to assess whether LSD1 is a  $\beta$ -catenin demethylase. A methylated  $\beta$ -catenin peptide encompassing lysine 180 ( $\beta$ -CAT K180Me) was incubated with recombinant LSD1 or with cellular extracts of HEK 293T cells overexpressing WT LSD1 or catalytically inactive LSD1 mutants (LSD1K661A and LSD1 K661A/W754A/Y761S,<sup>23</sup>). As shown in Fig. 4e, recombinant LSD1 and overexpressed WT LSD1 efficiently demethylated the  $\beta$ -cat K180Me peptide. Conversely, the catalytically inactive LSD1 mutants failed to demethylate the  $\beta$ -cat K180Me peptide. These results demonstrated that  $\beta$ -catenin is a non-histone substrate of LSD1 demethylase activity.

## Discussion

Using molecular and genetic approaches, we have demonstrated that in MuSCs  $\beta$ -catenin and LSD1 act together to promote asymmetric division and to activate the Core Enhancer of *MyoD*, thereby promoting myogenesis. The Wnt/ $\beta$ -Catenin pathway plays a key role in cell fate determination during development and in adult tissue regeneration by stem cells. These processes are complex and involve profound gene expression and epigenomic remodeling. Understanding the molecular mechanisms that relay and fine tune Wnt/ $\beta$ -Catenin signaling in cell fate determination has been a challenge over the past decades. Here we have identified a new check point of Wnt/ $\beta$ -Catenin signaling by showing that once in the nucleus  $\beta$ -Catenin must be demethylated by LSD1 to prevent its degradation via the proteasome.

It has been recently demonstrated that in myoblast cultures, LSD1 inhibition could promote the switch of myogenic cells into brown adipocytes in pro-adipogenic conditions <sup>24</sup>. Our results indicate that in pro-myogenic conditions, MuSCs, lacking LSD1, do not lose their myogenic identity. Similarly, *in vivo* LSD1 inactivation did not induced adipogenesis. Both genetic inactivation and the pharmacological inhibition of LSD1 led to a significative expansion of PAX7+ MuSCs after muscle injury, which remained fully myogenic even after repeated injuries.

Altogether, our results identify LSD1 essential in the canonical Wnt/ $\beta$ -catenin pathway, required for transcriptional regulation by  $\beta$ -catenin during MuSC commitment (Fig. 4f). It will be important in the future to determine whether the requirement of LSD1 for transcriptional regulation by  $\beta$ -catenin also applies to non-myogenic lineages.

## Acknowledgments

We thank Céline Anglereaux and Pierre Contard from the PBES in the SFR biosciences (UMS3444) for animal breeding. We thank T. Andrieu and S. Dussurgey from the AniRA-Cytometry platform in the SFR biosciences (UMS3444) for their expertise in cell sorting, and D. Ressnikoff and B. Chapuis (CIQLE imaging center, SFR Santé Lyon-Est (UMS3453) for their help with image acquisition. We also thank R. Mounier for critical reading the manuscript.

This study was funded by Association Francaise contre les Myopathies (AFM) through MyoNeurAlp alliance and by grant ANR-11-BSV2-017-01 and 'equipe FRM' grant from the Fondation pour le Recherche Medicale to L.S.

## Author Contributions

I.S. and L.S. conceived the research. S.M. and D.C. made *Lsd1* muscle specific inactivation. S.M. performed the CTX muscle injury. S.M., D.C. and F.B. performed immunofluorescence and histology on cryosections. F.L.G and N.R. contribute to Fig.1b. N.L. and I.S. performed the biochemical experiments. I.S. performed the myofiber cultures. I.S. wrote the manuscript with comments from all the authors.

## Declaration of interests

All the authors declare no conflict of interest.

## Methods

### Experimental model and subject details

#### Animals

All procedure on animals were performed in accordance with European regulations on animal experimentation and were approved by the local animal ethics committee (CECCAPP, University of Lyon) under the reference Apafis#16930. Mice were bred and housed in AniRA-PBES animal facility. They were maintained in a temperature- and humidity- controlled facility with a 12h light/dark cycle, free access to water and standard rodent show.

Nine-week-old C57BL/6J mice were purchased from Charles River laboratories and intraperitoneal injected with OG-L002 20mg/kg or NaCl 0,9% for 7 days.

The *Lsd1*<sup>tm1Schüle 25</sup> and *Pax7-CreERT2*<sup>26</sup> were previously described. Mice were genotyped with conventional PCR using standard conditions.

Allelic recombination under the *Pax7-CreERT2* allele was induced by intraperitoneal injections of 2mg of Tamoxifen (TAM) for 5 days.

Skeletal muscle injury was induced by an injection of 50 µl of cardiotoxin (10µM) into hindlimb TA muscle using 30G syringes under anesthesia induced by intraperitoneal injection with Ketamine (100mg/kg) and Xylazine (10mg/kg) in sterile saline solution. EdU solution (200µg) was injected intraperitoneally 12 hours before sacrifice.

#### Cell lines

C2C12 mouse myoblasts were maintained as myoblasts in growth medium (GM): Dulbecco's modified Eagle's medium supplemented with 15% fetal calf serum and antibiotics. Adult primary MuSCs were maintained on Matrigel-coated dishes in GM: Dulbecco's modified Eagle's medium F12 supplemented with 20% horse serum, 5 ng/mL fibroblast growth factor (FGF), and antibiotics. C2C12 cells and adult primary MuSCs were differentiated into myotubes by replacing GM with a myogenic differentiation medium containing 2% horse serum with antibiotics (MDM). HEK 293T cells were cultured using standard methods (ATCC).

## Methods details

### MuSC isolation

Adult primary MuSCs were isolated from skeletal muscle tissue as previously described<sup>27</sup>. Digested tissue was stained using antibodies: 0.2µg PE-conjugated rat anti-mouse CD31, 0.2µg PE-conjugated rat anti-

mouse CD45, 0.2µg PE-conjugated rat anti-mouse Sca-1, 5µg 647-conjugated rat anti-mouse integrin alpha7 and 2.5µg rat anti-mouse CD34. Cells were incubated with primary antibodies for 40 minutes on ice. Adult primary MuSCs were FACS isolated into MuSC medium based on cell surface antigen markers: CD31-/CD45-/Sca1-/integrin-α7+/CD34+ using a FACSAria III.

### **Myofiber culture**

We performed myofiber culture as described earlier<sup>28</sup>. Briefly, we carefully dissected Extensor Digitorum Longus (EDL) muscles and incubated them in DMEM (Gibco) containing 600U/ml of collagenase B for 75 min. The myofibers were dissociated by gentle trituration with a glass pipette. Myofibers were cultured for 42 h in DMEM containing 20% FBS and 5 ng/ml bFGF.

### **Cell treatments**

Inhibition of the proteasome was carried out by treating HEK 293T cells with MG132 at the indicated concentration and incubated for 6h at 37°C before the collection of cells. In protein degradation assays, protein synthesis was inhibited by the addition of cycloheximide (CHX) to C2C12 stable clones after 72h in MDM at a final concentration of 50 mg/ml in a time course before harvest, as indicated in the text. Canonical Wnt pathway activation was achieved by treating C2C12 stable clones and primary adult MuSCs with Wnt3a at 50 ng/ml or LiCl at 25mM for 6 h before the luciferase assay, proximity ligation assay, or RNA extraction. Inhibition of LSD1 enzymatic activity was carried out by treating primary adult MuSCs with Pargyline at 1mM and OG-L002 at 10µM for 72h in MDM. For proliferation assay EdU solution (20mM) has added to adult primary MuSCs for 2 hours before the collection of cells. Cells were analyzed using flow cytometry (FACS Cantoll).

### **Cell Transfection**

Different plasmids were transfected into C2C12 stable clones, MuSCs or HEK 293T with JetPRIME following provider's instruction for luciferase assays, immunoblotting, Co-IP, or Demethylase assay. To perform luciferase assays, C2C12 stable clones and primary adult MuSCs were grown in 6-well plates and cells in each well were co-transfected with 100 ng of TopFlash or FopFlash reporter plasmid and 1 ng of pRL-TK Renilla luciferase reporter. For immunoblotting analysis that was used for detecting the proteasome dependent degradation of β-Catenin protein and its mutant, 2 µg of pCMV β-Catenin WT or its mutant pCMV β-Catenin K180R were transfected into HEK 293T cells, which were cultured at about 70-80% confluency in 3.5 cm dishes. For Co-IP experiments, pCMV-LSD1 flag or pCMV β-Catenin or pCMV GFP were transfected into 70-80% confluent HEK 293T cells that were cultured in 15-cm culture dishes. For demethylase assay, 15cm plates containing 70-80% confluent HEK 293T cells were transfected with pCMV-LSD1 flag or pCMV-LSD1 K661A

flag or pCMV-LSD1 K661A W754A Y761A flag or pCMV-GFP (CTRL) after 24h incubation, protein extraction has been performed.

### **Luciferase assay**

C2C12 stable clones and primary adult MuSCs were transfected as previously described. After 24h, Wnt3A was added and incubated for another 6h at 37°C and luciferase activity was measured using the Dual-Luciferase Assay System. Each measurement was repeated with at least three independent transfections.

### **Immunoprecipitation**

Protein complexes were precipitated from nuclear fraction. Cell fractionation was performed as described <sup>29</sup>. 500µg of nuclear extracts from C2C12 stable clones, pCMV-LSD1 flag or pCMV-GFP transfected cells were incubated with specific antibodies coupled with beads or Flag beads in IP buffer (20mM HEPES pH7.5, 5mM K acetate, 0.5mM MgCl<sub>2</sub>, 0.5mM DTT, 150mM NaCl, 0.5% NP40 and Complete protease inhibitor) overnight at 4°C on a wheel. Beads were then washed 3 times in the IP buffer and resuspended in 1X loading sample buffer (IP buffer + 50mM Tris HCl pH 6.8, 10% glycerol, 100mM DTT, 2% SDS and bromophenol blue). Proteins were then loaded on a 4-15% SDS-PAGE transferred on a nitrocellulose membrane and blotted against the indicated antibodies.

### **Immunoblotting**

Cell fractionation was performed as described <sup>29</sup> and quantified using the DC protein assay (Bio-Rad). Nuclear extracts were separated by electrophoresis on 10% SDS-PAGE and transferred onto polyvinylidene fluoride (PVDF) Immobilon-P membranes. Immunoblots were revealed with enhanced chemiluminescence (ECL) PLUS reagent according to the manufacturer's instructions.

### **Immunofluorescence**

For plated MuSCs, 4 well Permanox chamber slides (Nunc Lab-Tek) were used and cells fixed with 4% (v/v) paraformaldehyde (PFA) for 10 minutes. Following fixation, material was permeabilized with 0.5% (v/v) Triton X-100 solution for 5 minutes and then blocked with 1% BSA, 0.2% Triton X-100 and 5% (v/v) goat serum for 60 minutes to reduce nonspecific antibody binding. Cells were then incubated with the following antibodies overnight at 4°C, 1:50 mouse anti-PAX7 (DSHB, clone PAX7), 1:50 mouse anti-Myogenin (DSHB, clone FD5), 1:50 mouse anti-MyHC (DSHB, clone A4.1025). Species-specific fluorochrome-conjugated secondary antibodies were then applied for 1 h at room temperature, before being mounted with 100 ng/ml of DAPI.

### **Chromatin immunoprecipitation (ChIP)**

ChIP experiments were carried out essentially as previously described <sup>3</sup>.

### ***In vitro* Demethylation assay**

HEK 293T cells were transfected with pCMV-LSD1 flag or pCMV-LSD1 K661A flag or pCMV-LSD1 K661A W754A Y761A flag or pCMV-GFP (CTRL). After 24h incubation, 4 mg of nuclear extracts were mixed with 40µl of Flag beads in IP buffer (20mM Tris Hcl pH8, 300mM NaCl, 0.5% NP40, 5% glycerol and Complete protease inhibitor during 3h at 4°C on a wheel. Beads were then washed 3 times in the IP buffer and eluted 2 times 90 min at 4°C on a wheel with 40µl of elution buffer (IP buffer + 150µg flag peptide). 15µl of each purification was used for the demethylase assay using 50µM (final concentration) of β-CAT WT peptide or β-CAT K180me peptide in 1X demethylase buffer (50mM Tris HCl pH8, 50nM FAD, 50mM NaCl, 5% glycerol, 20µg/ml BSA). 0.8µg of recombinant LSD1 (Sigma-Aldrich SRP0122) was used as positive control. After 1h at 37°C the reaction was stopped by adding sample loading buffer (final concentration 50mM Tris HCl pH 6.8, 10% glycerol, 100mM DTT, 2% SDS and bromophenol blue) and half of the reaction was loaded on a 4-20% precast gel. After transfer on a 0.2µm PVDF membrane proteins are detected with the indicated antibodies and with streptavidin coupled with HRP for the biotinylated peptides as loading control.

### **Real-Time qPCR**

Total RNA was isolated from cultured cells at 72h in MDM grown in 100-mm dishes using Trireagent. RNA was analyzed by real-time PCR using the QuantiFast SYBR Green PCR Kit. Relative gene expression was determined using the DCt method.

### **Proximity ligation Assay (PLA)**

Duolink® *in situ* PLA reagents were used to detect the interaction between β-catenin and BCL9 and the manufacturer's protocol was followed. Briefly, MuSCs, cultured on chamber slides to 40-50% confluence, were treated with Wnt3a (50ng/mL for 6 hours). Cells were treated with cytoskeleton buffer (PIPES 10mM, NaCl 100mM, Sucrose 300mM, MgCl<sub>2</sub> 3mM, EgTA 1mM and TrotonX100 0.5%), washed with PBS and then treated with cyto-stripping buffer (Tris-HCl 10mM, NaCl 10mM, MgCl<sub>2</sub> 3mM, Tween 40 1% and Sodium deoxycholate 0.5%) to remove the cytoplasm. Cells were then fixed, permeabilized and incubated overnight with mouse anti-β-catenin and rabbit anti-BCL9. The following day, cells were incubated with secondary antibodies conjugated to oligonucleotides (PLA probe PLUS and PLA probe MINUS) for 1 hour at 37°C. Afterward, ligation solution containing 2 oligonucleotides (that hybridize to the PLA probes) and Ligase was added for 30 minutes at 37°C. A closed circle is only formed if the 2 PLA probes are in close proximity. Finally, the closed circle was amplified using rolling-circle amplification reaction and the product was hybridized to fluorescently-labeled oligonucleotides. The fluorescent spots generated from positive interactions were quantified using a confocal microscope (Leica TCS SP5).

## Muscle Histology and immunohistochemistry

Mice were sacrificed and TA muscles were dissected and attached in Tragacanth gum, frozen in a cold 2-methylbutane bath and cryo-sectioned onto glass slides.

Tissue sections were freshly fixed with PFA 4% for 10 minutes, washed three washes in PBS, permeabilized in methanol for 6 minutes at -20°C and then washed three times in PBS. After 10 minutes incubation in a hot antigen retrieval buffer, sections were washed three times in PBS, 0,1% triton X-100 (PBS-T) and then were saturated 2 hours at room temperature with M.O.M Mouse IgG Blocking reagent. The antigen retrieval buffer contained 10mM sodium citrate acid and 0,05% tween-20 and was adjusted at pH 6,0. Tissue sections were washed once in PBS-T, incubated for 5 minutes in M.O.M diluent prepared according to the manufacturer and stained at 4°C overnight with primary antibodies diluted in M.O.M diluent (1/200 for anti-Ki67, 1/800 for anti-LSD1, 1/200 for anti-laminin, 1/50 for anti-Myogenin, 1/50 for anti-Pax7. Pax7 antibody has been obtained by concentrated 33 times the supernatant of the hybridoma's culture). After three 10 minutes washes in PBS-T, sections were incubated for 1 hour at room temperature with secondary antibody and DAPI diluted in M.O.M diluent. After three washes, sections were mounted with Fluoromount-G. Fluorescent images were acquired on a Zeiss Z1 Axioscan.

Hematoxylin and Eosin (H&E) and Oil Red O (ORO) staining were performed following standard methods.

## References

1. Wang, J. *et al.* Opposing LSD1 complexes function in developmental gene activation and repression programmes. *Nature* **446**, 882–887 (2007).
2. Pan, Y. C. *et al.* Wnt3a signal pathways activate MyoD expression by targeting cis-elements inside and outside its distal enhancer. *Biosci Rep* **35**, (2015).
3. Scionti, I. *et al.* LSD1 Controls Timely MyoD Expression via MyoD Core Enhancer Transcription. *Cell Rep* **18**, 1996–2006 (2017).
4. Robinson, D. C. L. & Dilworth, F. J. Epigenetic Regulation of Adult Myogenesis. *Curr. Top. Dev. Biol.* **126**, 235–284 (2018).
5. Yoshida, N., Yoshida, S., Koishi, K., Masuda, K. & Nabeshima, Y. Cell heterogeneity upon myogenic differentiation: down-regulation of MyoD and Myf-5 generates 'reserve cells'. *J. Cell. Sci.* **111** ( Pt 6), 769–779 (1998).
6. Zammit, P. S. Function of the myogenic regulatory factors Myf5, MyoD, Myogenin and MRF4 in skeletal muscle, satellite cells and regenerative myogenesis. *Semin. Cell Dev. Biol.* **72**, 19–32 (2017).

7. Zammit, P. S. *et al.* Muscle satellite cells adopt divergent fates: a mechanism for self-renewal? *J. Cell Biol.* **166**, 347–357 (2004).
8. Asakura, A. *et al.* Increased survival of muscle stem cells lacking the MyoD gene after transplantation into regenerating skeletal muscle. *Proc. Natl. Acad. Sci. U.S.A.* **104**, 16552–16557 (2007).
9. Rudolf, A. *et al.*  $\beta$ -Catenin Activation in Muscle Progenitor Cells Regulates Tissue Repair. *Cell Rep* **15**, 1277–1290 (2016).
10. Judson, R. N. *et al.* Inhibition of Methyltransferase Setd7 Allows the In Vitro Expansion of Myogenic Stem Cells with Improved Therapeutic Potential. *Cell Stem Cell* **22**, 177–190.e7 (2018).
11. Liang, Y. *et al.* A Novel Selective LSD1/KDM1A Inhibitor Epigenetically Blocks Herpes Simplex Virus Lytic Replication and Reactivation from Latency. *mBio* **4**, e00558-12 (2013).
12. Rodgers, J. T. *et al.* mTORC1 controls the adaptive transition of quiescent stem cells from G0 to G(Alert). *Nature* **510**, 393–396 (2014).
13. Siegel, A. L., Kuhlmann, P. K. & Cornelison, D. Muscle satellite cell proliferation and association: new insights from myofiber time-lapse imaging. *Skeletal Muscle* **1**, 7 (2011).
14. Kuang, S., Kuroda, K., Le Grand, F. & Rudnicki, M. A. Asymmetric self-renewal and commitment of satellite stem cells in muscle. *Cell* **129**, 999–1010 (2007).
15. Chai, Y. *et al.* Wnt signaling polarizes cortical actin polymerization to increase daughter cell asymmetry. *Cell Discov* **8**, 22 (2022).
16. Kaur, S. *et al.* Wnt ligands regulate the asymmetric divisions of neuronal progenitors in *C. elegans* embryos. *Development* **147**, dev183186 (2020).
17. Sun, Z. *et al.* Joint single-cell multiomic analysis in Wnt3a induced asymmetric stem cell division. *Nat Commun* **12**, 5941 (2021).
18. Junyent, S. *et al.* Wnt- and glutamate-receptors orchestrate stem cell dynamics and asymmetric cell division. *Elife* **10**, e59791 (2021).
19. Garcin, C. L. & Habib, S. J. A Comparative Perspective on Wnt/ $\beta$ -Catenin Signalling in Cell Fate Determination. in *Asymmetric Cell Division in Development, Differentiation and Cancer* (eds. Tassan, J.-P. & Kubiak, J. Z.) 323–350 (Springer International Publishing, 2017). doi:10.1007/978-3-319-53150-2\_15.
20. Kramer, T., Schmidt, B. & Lo Monte, F. Small-Molecule Inhibitors of GSK-3: Structural Insights and Their Application to Alzheimer's Disease Models. *Int J Alzheimers Dis* **2012**, 381029 (2012).

21. Brack, A. S. *et al.* BCL9 is an essential component of canonical Wnt signaling that mediates the differentiation of myogenic progenitors during muscle regeneration. *Dev Biol* **335**, 93–105 (2009).
22. Shen, C. *et al.* SET7/9 regulates cancer cell proliferation by influencing  $\beta$ -catenin stability. *FASEB J.* **29**, 4313–4323 (2015).
23. Lee, M. G. *et al.* Functional interplay between histone demethylase and deacetylase enzymes. *Mol Cell Biol* **26**, 6395–6402 (2006).
24. Tomic, M. *et al.* Lsd1 regulates skeletal muscle regeneration and directs the fate of satellite cells. *Nat Commun* **9**, 366 (2018).
25. Zhu, D. *et al.* Lysine-specific demethylase 1 regulates differentiation onset and migration of trophoblast stem cells. *Nat Commun* **5**, 3174 (2014).
26. Lepper, C., Conway, S. J. & Fan, C.-M. Adult satellite cells and embryonic muscle progenitors have distinct genetic requirements. *Nature* **460**, 627–631 (2009).
27. Liu, L., Cheung, T. H., Charville, G. W. & Rando, T. A. Isolation of skeletal muscle stem cells by fluorescence-activated cell sorting. *Nat Protoc* **10**, 1612–1624 (2015).
28. Pasut, A., Jones, A. E. & Rudnicki, M. A. Isolation and culture of individual myofibers and their satellite cells from adult skeletal muscle. *J Vis Exp* e50074 (2013) doi:10.3791/50074.
29. Martini, E., Roche, D. M., Marheineke, K., Verreault, A. & Almouzni, G. Recruitment of phosphorylated chromatin assembly factor 1 to chromatin after UV irradiation of human cells. *J Cell Biol* **143**, 563–575 (1998).

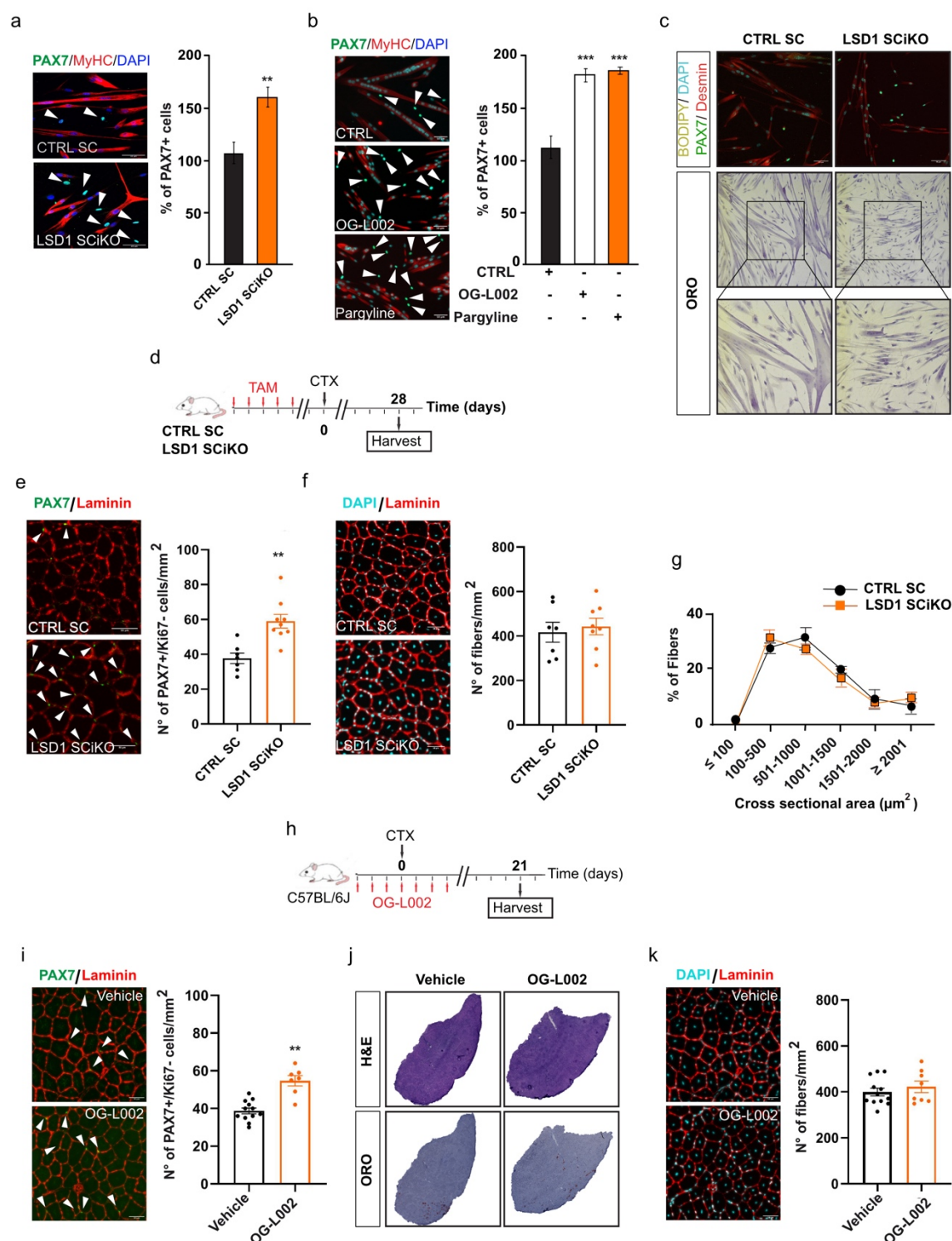


**Fig. 1 LSD1 regulates MuSC self-renewal potential.** **a**, PAX7 and MyHC staining and percentage of PAX7+/Ki67- cells after 48 h under myogenic differentiation conditions of CTRL SC and LSD1 SCiKO MuSCs. **b**, PAX7 and MyHC staining and percentage of PAX7+/Ki67- cells after 48 h under myogenic differentiation conditions of MuSCs treated with LSD1 inhibitors (OG-L002 and Pargyline). **c**, Bodipy, PAX7, desmin and Oil Red O staining of cells after 48 h under myogenic differentiation conditions of

CTRL SC and LSD1 SCiKO MuSCs. **d**, CTX experimental setup. **e**, Anti-PAX7 and anti-Laminin staining on cryosections of regenerated TA muscles in CTRL SC and LSD1 SCiKO mice at 28 dpi. Quantification of the number of sublamina PAX7+/Ki67- cells per mm<sup>2</sup>. **f**, Anti-Laminin staining on cryosections of regenerated TA muscles in CTRL SC and LSD1 SCiKO mice at 28 dpi. Quantification of the number of myofibers per mm<sup>2</sup>. **g**, CSA distribution of muscle fibers in CTRL SC and LSD1 SCiKO mice TA cryosections at 28 dpi. **h**, CTX experimental setup. **i**, Anti-PAX7 and anti-Laminin staining on cryosections of regenerated TA muscles in Vehicle and OG-L002 treated mice at 21 dpi. Quantification of the number of sublamina PAX7+/Ki67- cells per mm<sup>2</sup>. **j**, H&E and Oil Red O staining on cryosections of regenerated TA muscles in Vehicle and OG-L002 treated mice at 21 dpi. **k**, Anti-Laminin staining on cryosections of regenerated TA muscles in Vehicle and OG-L002 treated mice at 21 dpi. Quantification of the number of myofibers per mm<sup>2</sup>.

Scale bars, 50  $\mu$ m. n = 3 mice/genotype. n = 3 primary MuSC cultures/genotype. n = 3 primary MuSC cultures/treatments. Values are mean or percentage mean  $\pm$  SEM. \*\*p < 0.01, \*\*\*p < 0.001 (Bonferroni test after one way-ANOVA).

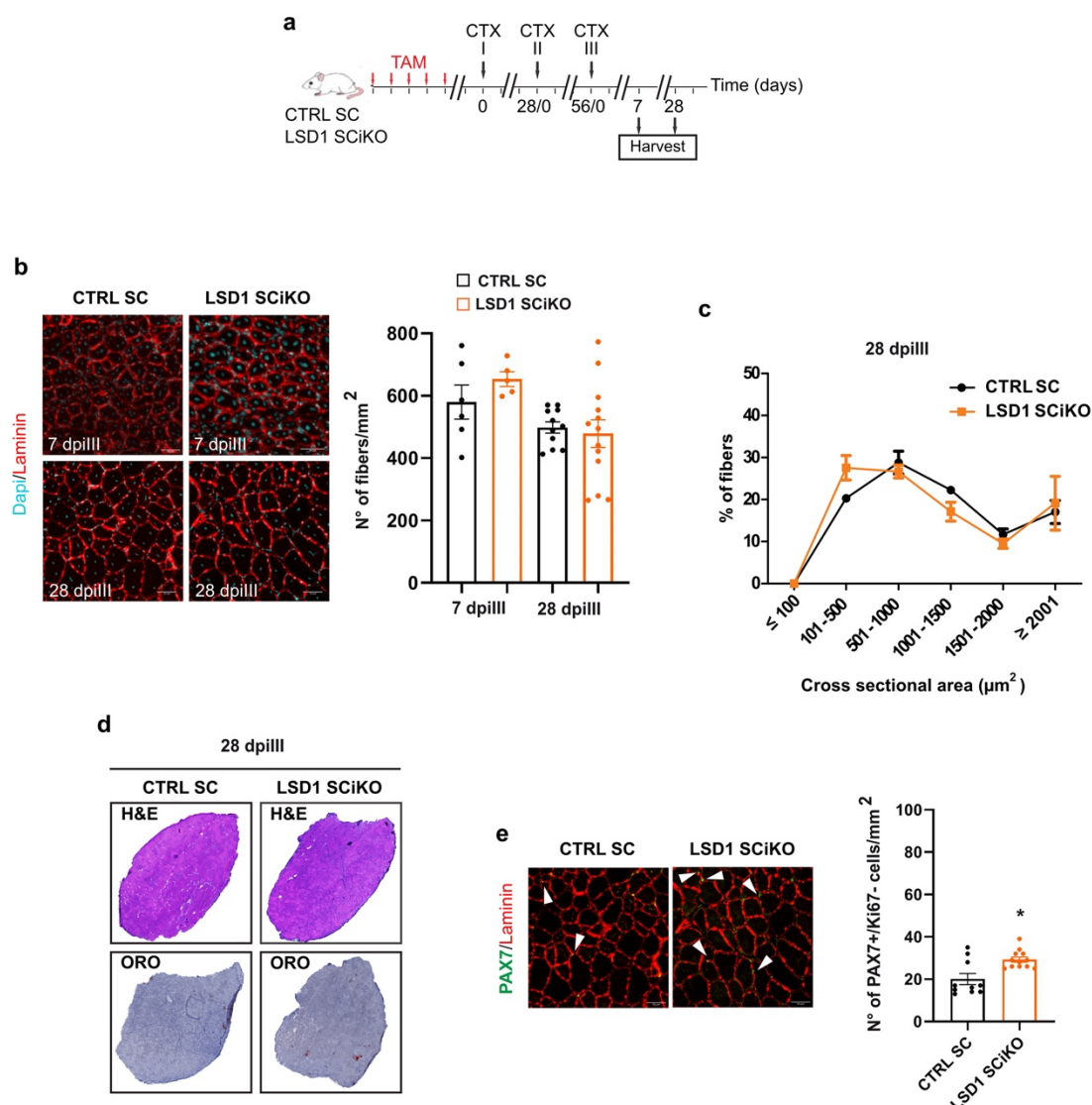


**Fig. 2 LSD1 SCiKO MuSCs maintain their regenerative potential after repeated injuries.** **a**, Repeated CTX experimental setup. **b**, Laminin staining on cryosections of regenerated TA muscles in CTRL SC and LSD1 SCiKO mice at 7 and 28 dpi. Quantification of the number of myofibers per mm<sup>2</sup>. **c**, CSA distribution of muscle fibers in CTRL SC and LSD1 SCiKO mice TA cryosections at 28 dpi. **d**, H&E and Oil Red O staining on cryosections of regenerated TA muscles in CTRL SC and LSD1 SCiKO mice at 28 dpi. **e**, Anti-PAX7 and anti-Laminin staining on cryosections of regenerated TA muscles in CTRL SC and LSD1 SCiKO mice at 28 dpi. Quantification of the number of sublaminal PAX7+/Ki67+ cells per mm<sup>2</sup>.

Scale bars, 50 μm. n = 5 mice/genotype. Values are mean ± SEM. \*p < 0.05 (Bonferroni test after one way-ANOVA).

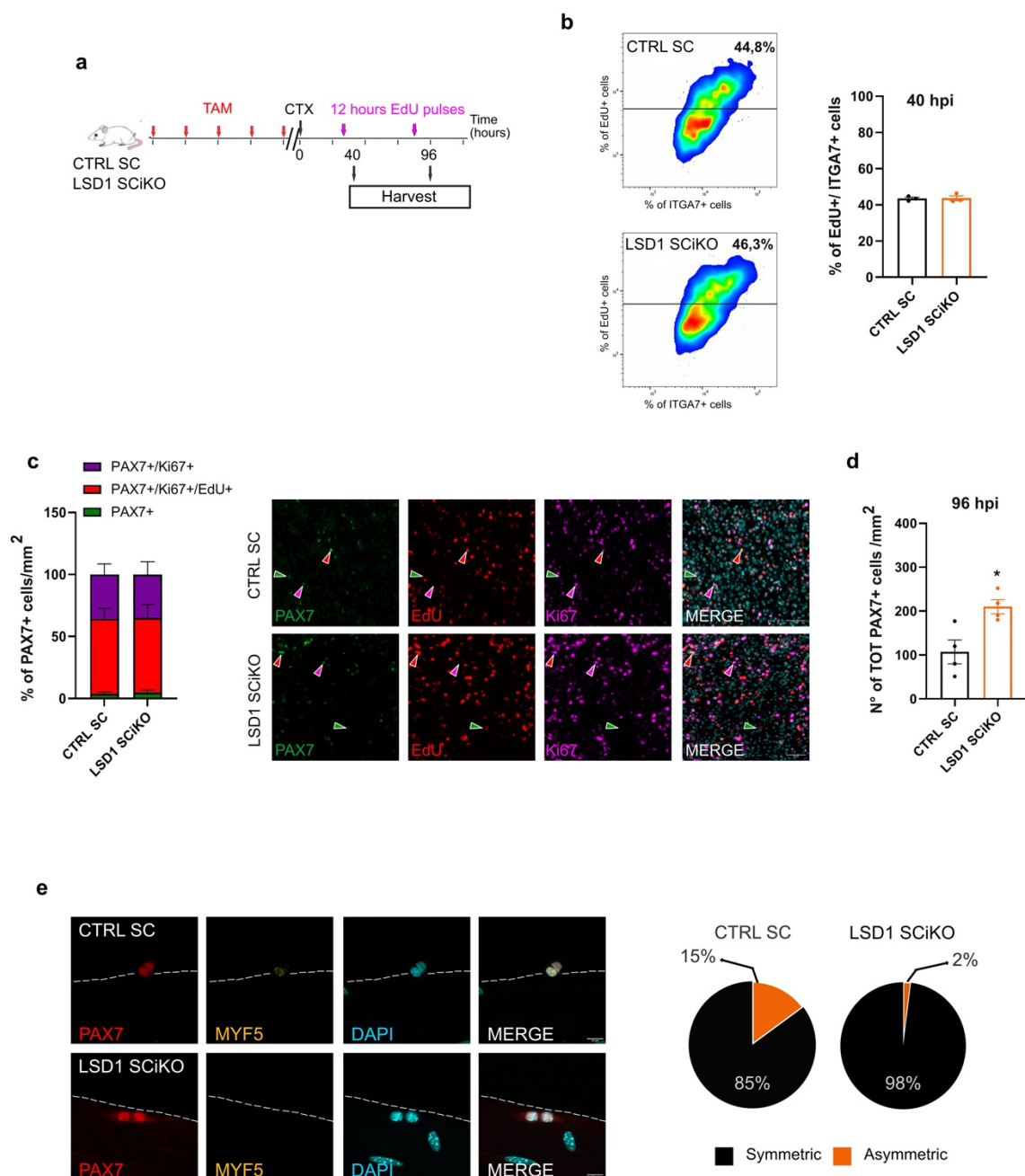


**Fig. 3 Lack of LSD1 stimulates symmetric division.** **a**, EdU pulse labelling set up. **b**, FACS-acquired quantification of EdU+ MuSCs (ITGA7+) isolated from muscle 40 h post injury (hpi). **c**, Percentage of PAX7+/Ki67+ (violet), PAX7+/Ki67+/EdU+ (red) and PAX7+/Ki67-/EdU- (green) MuSCs at 96hpi was quantified per mm<sup>2</sup>. Representative images of PAX7, Ki67 and EdU staining on cryosections of regenerated TA muscles. **d**, Quantification of the total number of PAX7+ cells at 96 hpi per mm<sup>2</sup>. **e**, Anti MYF5 and PAX7 staining on EDL myofibers isolated from CTRL SC and LSD1 SCiKO mice and cultured for 42 hours. MuSCs either give rise to one PAX7+/MYF5- stem cell and one PAX7+/MYF5+ committed

cell, via asymmetric cell division, or alternatively give rise to two MYF5- daughter cells by symmetric cell division.

Scale bars, 50  $\mu\text{m}$  and 10  $\mu\text{m}$ . n = 3 mice/genotype for **(b)**, **(c)** and **(d)** panels. n = 6 mouse/genotype for **(e)** panel. Values are mean or percentage mean  $\pm$  SEM. \*p < 0.05 (Bonferroni test after one way-ANOVA).

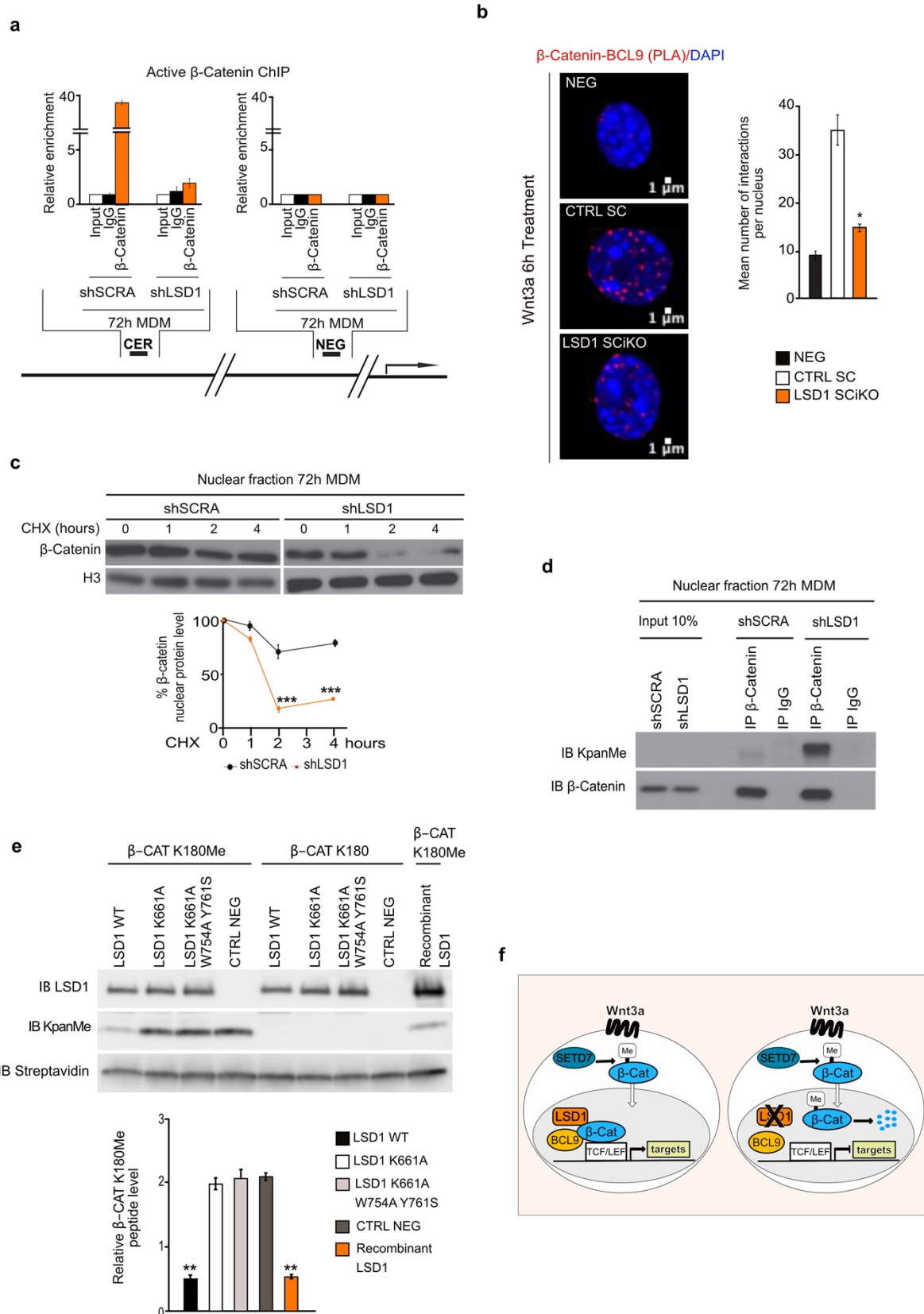


**Fig. 4 LSD1 demethylates  $\beta$ -catenin protein.** **a**, Localization of  $\beta$ -catenin at the Core Enhancer region (CER) of *MyoD* gene locus after 72 h in myogenic differentiation medium (MDM). ChIP analysis was

performed on shSCRA and shLSD1 cells with an anti- $\beta$ -catenin antibody. Enrichment values were shown as fold difference relative to the NEG region. **b**, BCL-9 and  $\beta$ -catenin protein-protein interactions evaluated using *in situ* proximity ligation assay (PLA). Complexes visualized as red dots. Scale bar, 1  $\mu$ m. Quantification of BCL-9/  $\beta$ -catenin PLA assay on CTRL SC and LSD1 SCiKO cells after 6 h of Wnt3A treatment. Red dots were quantified in nucleus from at least 100 cells per condition. **c**, LSD1 knockdown accelerated the turnover rate of endogenous  $\beta$ -catenin in shSCRA and shLSD1 cells after 72 h in MDM, in a time-course CHX treatment. **d**, Loss of LSD1 function caused an increase in methylated  $\beta$ -catenin protein in the nucleus after 72 h in MDM. **e**, Demethylation assay using methylated and non-methylated lysine 180  $\beta$ -catenin peptides as substrate. LSD1 WT, LSD1 K661A and LSD1 K661A/W754A/Y761S and commercial recombinant LSD1 were incubated with  $\beta$ -CAT K180Me and  $\beta$ -CAT K180 and analyzed by western blot with anti KpanMe antibody. The streptavidin antibody was used to detect the  $\beta$ -catenin peptides, which were conjugated to biotin. **f**, Representative schema of the LSD1 and canonical Wnt pathway interplay hypothesis.

Values are mean of at least three experiments.  $\pm$  SEM. \* $p < 0.05$ , \*\* $p < 0.01$ , \*\*\* $p < 0.001$  (Bonferroni test after one way-ANOVA).